# Anomalous Lattice Dynamics near the Ferroelectric Instability in PbTe

Yi Zhang,[1] Xuezhi Ke,[2,1] Paul R. C. Kent,[3] Jihui Yang,[4] and Changfeng Chen[1]

[1]*Department of Physics and HiPSEC, University of Nevada, Las Vegas, Nevada 89154, USA*
[2]*Department of Physics, East China Normal Univeristy, Shanghai 200062, China*
[3]*Center for Nanophase Materials Sciences, Oak Ridge National Laboratory, Oak Ridge, Tennessee 37831, USA*
[4]*Materials Science and Engineering Department, University of Washington, Seattle, Washington 98195, USA*

A recent report of highly unusual ferroelectric fluctuations in PbTe by E. S. Božin *et al.* [Science **330,** 1660 (2010)] raises fundamental questions about the nature of underlying lattice dynamics. We show by first-principles calculations that the reported results can be attributed to abnormally large-amplitude thermal vibrations that stem from a delicate competition of dual ionicity and covalency, which puts PbTe near ferroelectric instability. It produces anomalous properties such as partially localized low-frequency phonon modes, a soft transverse optical phonon mode, and a positive temperature coefficient for the band gap. These results account for experimental findings and resolve the underlying atomistic mechanisms, which have broad implications for materials near dynamic instabilities.

　　　　PACS numbers: 63.20.−e, 71.20.−b, 72.15.Jf

Knowledge of lattice dynamics is essential to understanding the fundamental physics of solids [1]; it reveals the nature of atomic bonding and electron-phonon interaction that determine material properties. A recent neutron diffraction experiment [2] unveiled a striking tendency toward stronger ferroelectric fluctuations in PbTe on heating, which is highly unusual, since rising temperature normally drives materials away from ferroelectric instability. Another recent experiment [3] reported giant anharmonic phonon scattering in PbTe. These intriguing phenomena raise fundamental questions about the underlying lattice dynamics and its role in determining the phonon and electronic properties of lead chalcogenides. Past studies [4–11] have unveiled interesting physics concerning PbTe and its nanocomposites. However, previous standard phonon calculations were unable to capture the anomalies seen in the latest experiments [2,3]. It underscores the urgency of establishing a microscopic understanding of these new phenomena.

In this Letter, we report on a theoretical study aimed at unraveling the atomistic mechanisms underlying the anomalous properties of PbTe. We show by first-principles molecular dynamics (MD) simulations that the experimentally observed broadening and non-Gaussian deviation of pair distribution function (PDF) peaks on heating [2] can be attributed to abnormally large-amplitude thermal vibrations; our results demonstrate that the system does not contain any stabilized local dipole moment, despite its proximity to ferroelectric instability. Our phonon calculations identify partially localized low-frequency phonon modes and a soft transverse optical phonon mode, which result from unusually shallow or highly anharmonic potential wells. These anomalies stem from the competing ionicity and covalency that put PbTe in the close vicinity of a dynamic (ferroelectric) instability. Our first-principles electronic structure cal-

culations show considerable band-gap variations associated with individual phonon modes, which account for the experimentally observed positive temperature coefficient of the band gap. These results offer insights into the intriguing properties of lead chalcogenides and broaden our understanding of the general topic of phonon and electronic properties of materials near dynamic instabilities.

We first study the PDF spectrum by MD simulations using the VASP package [12] and a cubic supercell containing 216 atoms with dimensions of $(19.67 \text{ Å})^3$. A grand canonical ensemble is simulated using the Nosé algorithm [13]. A preliminary equilibrating simulation is first performed for 8 ps with a time step of 2 fs. The simulation is then performed for 12 ps. The PDF spectrum for each time step is collected, and the results are then averaged to obtain the overall PDF, as shown in Fig. 1. Our simulations reproduce all the major experimental findings reported in Ref. [2]. First, the PDF peaks broaden considerably, while their peak maxima drop significantly with rising temperature [Fig. 1(a)]. In particular, the nearest-neighbor PDF peak broadens, and its maximum drops as rapidly as those of the higher-neighbor peaks. This striking result indicates unusually large atomic displacements in PbTe. Secondly, all the PDF peaks deviate from Gaussian distribution at high temperatures. Figure 1(c) shows the nearest-neighbor peak at 500 K with a non-Gaussian deviation and an intensity increase on the high-$r$ side; these anomalies are absent at low temperatures [e.g., the 50 K result shown in Fig. 1(b)]. Furthermore, PDFs constructed from static displacement calculations show that the [001]-PbO distorted structure [2] induces the most peak broadening (compared to those of the structures with [000], [001], or [111] distortion), thus providing the best fit to the MD (and experimental) results. The critical issue now is to identify the atomistic mechanism for these novel phenomena.
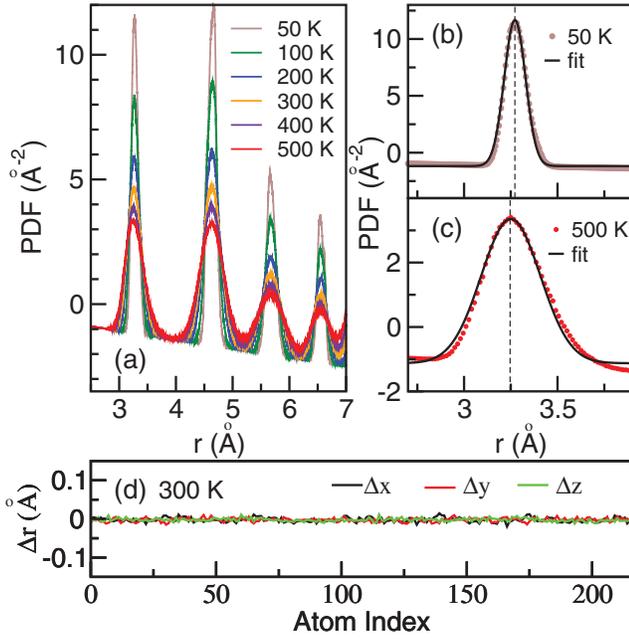
FIG. 1 (color).   (a) The calculated PDFs of PbTe. (b),(c) The nearest-neighbor PDF peaks at 50 and 500 K with Gaussian fittings. (d) Average displacements of all atoms in the supercell during the simulation (12 ps).

It has been suggested [2] that the anomalous PDF results may indicate stable local dipole formation in PbTe at elevated temperatures. To resolve this issue, we evaluate the atomic displacements in the supercell, and the results are negligibly small at all temperatures [Fig. 1(d) shows data at 300 K]. It demonstrates that PbTe does not harbor *stable* local dipole formation; instead, the atoms undergo large-amplitude thermal vibrations. Our results show pronounced root-mean-square displacements of 0.159 and 0.122 Å at 300 K for Pb and Te, respectively, which are comparable to those of weakly bonded "rattling" atoms in skutterudites [14]. Such large thermal displacements, increasing with rising temperature, perturb the interatomic distances significantly, thus broadening the PDF peaks. Here, the crystal structure remains undistorted on average; as an atom vibrates around its original position, its average pair distance to neighboring atoms is increased due to the reduced crystal symmetry, leading to an increase of the high-$r$ part of the PDF peaks. This increase is negligible in most materials with normal vibrational amplitudes. In PbTe, however, the abnormally large-amplitude vibrations produce detectable non-Gaussian PDF peaks on heating as observed in an experiment [2] and our MD simulations.

We calculated phonon dispersions of PbTe (using an 8-atom cubic cell) by the direct force-constant method as implemented in PHONON software [15] (technical details are described elsewhere [9]). The numerical stability has been verified by extensive convergence tests on $k$ points, cutoff, and supercell size. Our calculated phonon dispersions agree well with previous work using linear response
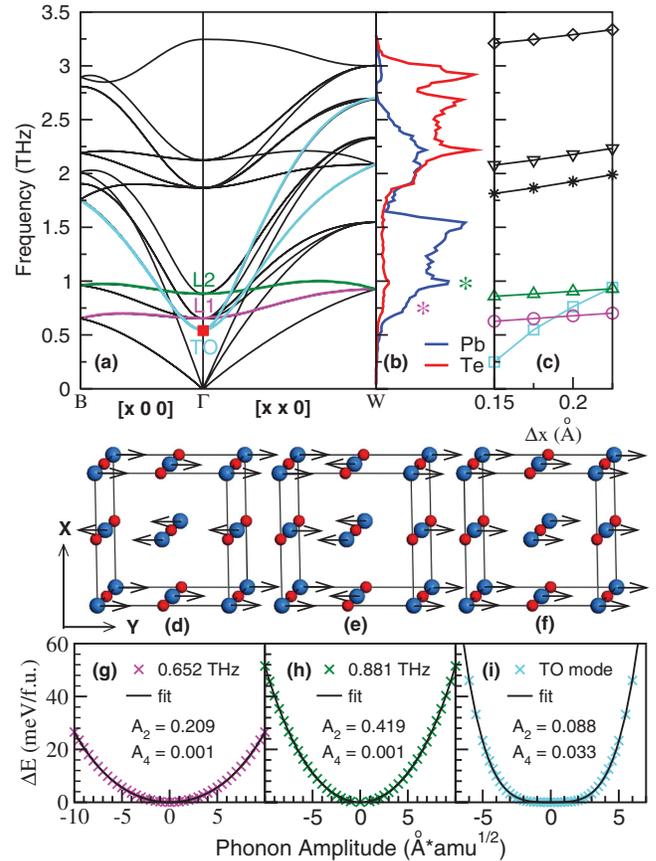


FIG. 2 (color).   (a) Calculated phonon dispersion of PbTe. Two partially localized low-frequency branches (L1 and L2) and a soft TO mode are labeled. The red square denotes the experimental TO frequency at the $\Gamma$ point [30], which perfectly matches the calculated result. (b) Partial phonon density of states. (c) The frequency variation of the phonon modes at the $\Gamma$ point versus the atomic displacement used in the phonon calculations. (d)–(f) Atomic displacements (only Pb motions are shown for clarity) of L1, L2, and TO modes at the $\Gamma$ point. (g)–(i) Potential energy curves as a function of phonon amplitude $Q_{\Gamma,i}$, defined as $\mathbf{U}_{i,j} = Q_{\Gamma,i}/\sqrt{M_j}\,\mathbf{e}_{i,j}$, where $\mathbf{U}$, $\mathbf{e}$, and $M$ are the displacement vector, polarization vector, and atomic mass, respectively. They are fitted by a fourth-order polynomial $y = A_2 x^2 + A_4 x^4$.

theory [8]. The unusually large thermal displacements and heavy atomic mass generate anomalously low-frequency phonon modes in PbTe. Two nearly localized optical phonon branches are identified between $B(0.5, 0, 0)$-$\Gamma$ and $\Gamma$-$W(0.5, 0.5, 0)$ [Fig. 2(a)]; their frequencies at the $\Gamma$ point are only 0.652 and 0.881 THz. Nevertheless, dispersions are found along $\Gamma$-$L(0.5, 0.5, 0.5)$, indicating that these modes are partially localized. These low-frequency and partially localized phonon modes are responsible for the Pb-dominated peak at ~1 THz and peak shoulders at lower frequencies in the phonon density of states [Fig. 2(b)]. This is analogous to the behavior of the rattling mode in a variety of filled cage compounds [16,17] and $Zn_4Sb_3$ [18]

that are known as "phonon-glass" materials. As a result, strong phonon scattering is expected from the interaction of the acoustic heat-transporting phonons with the partially localized modes that are low in energy to cross the acoustic branches. A distinctive feature here is that the phonon modes in PbTe are collective due to the high symmetry of PbTe structure, which is different from the localized atomic [16,17] or dumbbell-like [18] vibrations. The two-fold degenerate phonon branch of 0.548 THz at the $\Gamma$ point is a soft transverse optical (TO) mode, which is closely related to the incipient ferroelectricity of PbTe [19] and the giant anharmonic scattering with the longitudinal acoustic mode [3]. The TO frequency at the $\Gamma$ point exhibits strong dependence on the choice of atomic displacement in phonon calculations [Fig. 2(c)]. Therefore, an increase of TO frequency is expected when the thermal amplitude becomes larger, which qualitatively explains the origin of the TO hardening on increasing temperature [20].

The partially localized vibrational modes at the $\Gamma$ point are dominated by relative shear and compressive motions of Pb atoms in two different (001) layers [Figs. 2(d) and 2(e)]. These modes are only weakly coupled with the wave vector when the wave propagation direction is normal to the vibrational direction, causing the nearly $k$-independent dispersion. Meanwhile, as shown in Fig. 2(f), the soft TO mode corresponds to the motion of all Pb atoms in one direction, while the Te atoms are moving in the opposite direction. The independent potential energy surfaces of the three phonon modes at $\Gamma$ as functions of the normal mode amplitude $Q_{\Gamma,i}$ are shown in Figs. 2(g)–2(i). These shallow potential wells are consistent with previous calculations [21]; they are the underlying cause of the large thermal vibrations and low-frequency phonon modes. In particular, the interlayer interactions for the shear mode are small, resulting in the shallowest potential well in Fig. 2(g). The potential wells for two partially localized modes are nearly parabolic and are thus harmonic. However, the U-shaped potential well for the TO mode is highly anharmonic, which favors the scattering between the TO and other phonon modes and could be responsible for the large Grüneisen parameter and anomalous thermal expansion in PbTe [9]. The flat well bottom indicates that large-amplitude vibrations can be excited at low temperatures.

In lead chalcogenides and many $A^N B^{8-N}$ octet semiconductors, it is a generic feature that covalency coexists with ionicity, which dominates phonon properties (and potential surfaces) [22] and causes instability of shear-type localized phonon modes under compression [9]. Figure 3 shows the results of a comparative study of the electron charge density of cubic PbTe, NaCl, and GeTe at equilibrium or when the ions are displaced in the TO-mode manner along the $\langle 001 \rangle$ and $\langle 011 \rangle$ directions. NaCl is purely ionic with all the charge accumulated on Cl anions. For PbTe and GeTe, charge is present both on ions and in the space between cation and anion. A Bader charge
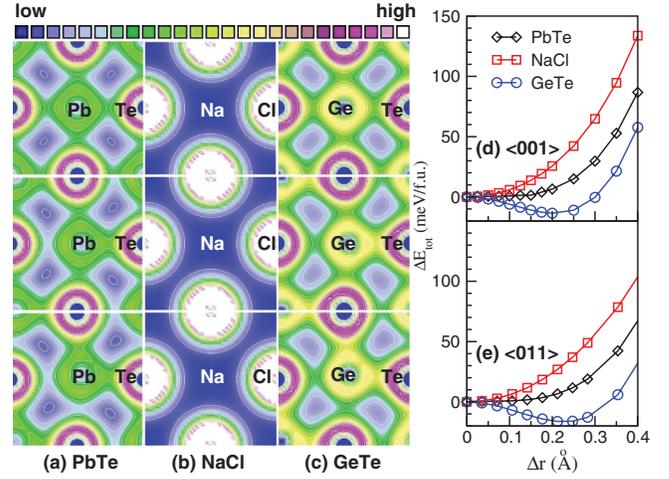


FIG. 3 (color).   The charge density of cubic (a) PbTe, (b) NaCl, and (c) GeTe in the (001) plane at equilibrium (top row), with the ions displaced along the $\langle 001 \rangle$ (middle) and $\langle 011 \rangle$ (bottom) directions by 0.2 Å. (d),(e) Energy surfaces for the $\langle 001 \rangle$ and $\langle 011 \rangle$ displacements.

analysis [23] obtains $3.28e$ and $6.72e$ for Pb and Te in PbTe and $3.68e$ and $6.32e$ for Ge and Te in GeTe, respectively. These are significant deviations from the nominal $2e$ and $8e$ for the 2+ cation and the 2− anion, and the actual bonding in both systems is partially covalent. The sixfold coordinated cubic structure is stabilized by the electrostatic Madelung energy; however, it is not favored by covalent characters which tend to form fourfold coordinated structures [22]. As atomic displacement occurs, more charge is accumulated in the compressed interatomic space along bonding directions to form short covalent bonds. This process competes with the electrostatic restoration energy and leads to different energy surfaces. No charge transfer is seen in distorted NaCl, leading to a steep harmonic potential well and a stable TO mode. GeTe is dynamically unstable, since the energy minimum moves $\sim 0.24$ Å away from $\Delta r = 0$. Meanwhile, PbTe is situated in between, being more covalent than NaCl but less so than GeTe. It remains dynamically stable but it is in the close vicinity of ferroelectric instability, where shallow potential wells and large anharmonicities take place. These results explain the incipient ferroelectricity of PbTe [19] and the rhombohedral phase transition of GeTe [24] at low temperatures. We also estimated the static dielectric permittivity of PbTe using our calculated phonon dispersion and the Lyddane-Sachs-Teller relation [25]; the obtained value of $\epsilon_0$ of around 1200 lies within the typical range for incipient ferroelectrics [26].

One of the most striking properties of PbTe is the anomalous positive temperature dependence of its fundamental band gap [5,6]. Here, we elucidate its connection to the unusual lattice vibrations. We performed electronic structure calculations using the generalized gradient approximation [27] implemented in VASP [12] and including
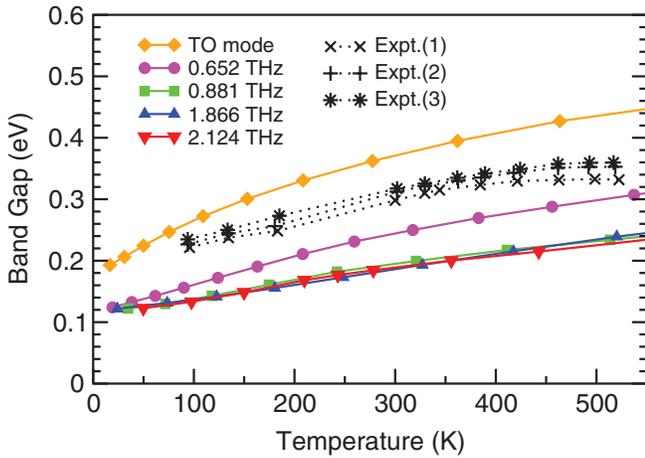
FIG. 4 (color). Band-gap variation with temperature for several phonon modes at the $\Gamma$ point. The experimental data [29] are shown for comparison.

the spin-orbit interaction. The projector-augmented-wave method [28] is used with a cutoff energy of 400 eV. We calculated band gaps associated with several low-frequency phonon modes. The energy of each phonon mode with frequency $\omega_i$ at temperature $T$ is given by $E_i = \hbar\omega_i(\frac{1}{2} + \frac{1}{e^{\hbar\omega_i/k_BT}-1})$. It is mapped onto the potential energy curves [e.g., Figs. 2(g)–2(i)] to extract the corresponding (average) atomic displacement. The band gaps are then calculated with these atomic displacements in the supercell, and the results (Fig. 4) all show the same trend in agreement with experimental data [29]; the quantitative variations can be attributed to the different extent of repulsion between Te $p$ and Pb $s$ orbitals [7] for different atomic displacements. The soft TO mode has the largest zero-point amplitude and it leads to the largest $dE_g/dT$ of 0.86 meV/K below 100 K and gradually decreases to 0.23 meV/K near 500 K, indicating the stronger electron-phonon interaction at low temperatures. These results establish a close relation between lattice dynamics and the electronic band gap in PbTe. While a more accurate description of the band gap requires a denser sampling of the Brillouin zone, our results unveil a new mechanism for the unusual band-gap variation driven by large atomic displacements.

In summary, we demonstrate by *ab initio* calculations that the anomalous lattice dynamics in PbTe stem from a delicate competition of ionicity and covalency that explains its incipient ferroelectricity. It leads to abnormally large-amplitude thermal vibrations and produces partially localized low-frequency phonon modes and a soft TO mode which, in turn, induce strong electron-phonon interaction and a positive temperature dependence of the band gap. The atomistic mechanisms unveiled here provide insights for understanding peculiar phonon and electronic properties of lead chalcogenides. The present results highlight distinct material behaviors and compel further

exploration of new physical phenomena near dynamic instabilities.

[1] J. M. Ziman, *Electrons and Phonons: The Theory of Transport Phenomena in Solids* (Clarendon, Oxford, 1960).
[2] E. S. Božin *et al.*, Science **330**, 1660 (2010).
[3] O. Delaire *et al.*, Nature Mater. **10**, 614 (2011).
[4] W. Cochran *et al.*, Proc. R. Soc. A **293**, 433 (1966).
[5] C. Keffer, T. M. Hayes, and A. Bienenstock, Phys. Rev. B **2**, 1966 (1970).
[6] Y. W. Tsang and M. L. Cohen, Phys. Rev. B **3**, 1254 (1971).
[7] S. H. Wei and A. Zunger, Phys. Rev. B **55**, 13605 (1997).
[8] A. H. Romero *et al.*, Phys. Rev. B **78**, 224302 (2008).
[9] Y. Zhang *et al.*, Phys. Rev. B **80**, 024304 (2009).
[10] X. Ke *et al.*, Phys. Rev. Lett. **103**, 145502 (2009).
[11] Y. Zhang *et al.*, Phys. Rev. Lett. **106**, 206601 (2011).
[12] G. Kresse and J. Furthmüller, Phys. Rev. B **54**, 11169 (1996). Our results are insensitive to the choice of density functionals PW91 or PBE; the PW91 results are shown.
[13] S. Nosé, J. Chem. Phys. **81**, 511 (1984).
[14] B. C. Chakoumakos *et al.*, Acta Crystallogr. Sect. B **55**, 341 (1999).
[15] K. Parlinski, Z.-Q. Li, and Y. Kawazoe, Phys. Rev. Lett. **78**, 4063 (1997).
[16] R. P. Hermann *et al.*, Phys. Rev. Lett. **90**, 135505 (2003).
[17] J. L. Cohn *et al.*, Phys. Rev. Lett. **82**, 779 (1999).
[18] W. Schweika *et al.*, Phys. Rev. Lett. **99**, 125501 (2007).
[19] B. T. Bate, D. L. Carter, and J. S. Wrobel, Phys. Rev. Lett. **25**, 159 (1970).
[20] H. A. Alperin *et al.*, Phys. Lett. **40A**, 295 (1972).
[21] J. An, A. Subedi, and D. J. Singh, Solid State Commun. **148**, 417 (2008).
[22] V. Ozoliņš and A. Zunger, Phys. Rev. Lett. **82**, 767 (1999).
[23] W. Tang, E. Sanville, and G. Henkelman, J. Phys. Condens. Matter **21**, 084204 (2009).
[24] K. M. Rabe and J. D. Joannopoulos, Phys. Rev. B **36**, 6631 (1987).
[25] R. H. Lyddane, R. G. Sachs, and E. Teller, Phys. Rev. **59**, 673 (1941).
[26] V. V. Lemanov *et al.*, Solid State Commun. **110**, 611 (1999).
[27] J. P. Perdew *et al.*, Phys. Rev. B **46**, 6671 (1992).
[28] G. Kresse and D. Joubert, Phys. Rev. B **59**, 1758 (1999).
[29] R. N. Tauber, A. A. Machonis, and I. B. Cadoff, J. Appl. Phys. **37**, 4855 (1966).
[30] G. Bauer *et al.*, in *Proceedings of the International Conference on Lattice Dynamics, Paris, 1977*, edited by M. Balkanski (Flammarion, Paris, 1978), p. 669.